

Adrenal lymphoma with hypertension: A report of three cases

KUNLEI TAN¹, ZHIJUN HAN^{2*}, YALI ZHOU^{2*}, MIDUO TAN³, LEI CHEN¹ and YINCHUN DENG⁴

¹Department of Urology, Zhuzhou Hospital Affiliated to Xiangya School of Medicine, Central South University, Zhuzhou, Hunan 412000, P.R. China; ²Department of Neonatology, Zhuzhou Hospital Affiliated to Xiangya School of Medicine, Central South University, Zhuzhou, Hunan 412000, P.R. China; ³Department of Breast Surgery, Zhuzhou Hospital Affiliated to Xiangya School of Medicine, Central South University, Zhuzhou, Hunan 412000, P.R. China; ⁴First Department of Colorectal and Anal Surgery, Digestive Disease Medical Center Zhuzhou Hospital Affiliated to Xiangya School of Medicine, Central South University, Zhuzhou, Hunan 412000, P.R. China

Received February 25, 2026; Accepted May 12, 2026

DOI: 10.3892/ol.2026.15685

Abstract. Adrenal lymphoma is a rare clinical entity, classified as either primary adrenal lymphoma (PAL) or secondary adrenal lymphoma. PAL is a highly aggressive malignancy with an extremely low incidence rate. To date, <250 cases have been reported in the English literature. The clinical manifestations of PAL are diverse and non-specific, often resulting in a delayed diagnosis or a misdiagnosis. In patients with comorbid hypertension, the differential diagnosis of an adrenal mass typically emphasizes functional tumors, such as aldosterone-producing tumors (which cause primary aldosteronism) and pheochromocytoma. Due to the usual absence of characteristic hormonal abnormalities, PAL is frequently overlooked in clinical practice. The present report describes the cases of 3 male patients with PAL, aged 83, 73 and 63 years. The first 2 patients had pre-existing hypertension prior to the confirmation of PAL. The present report summarizes the diagnostic strategies for PAL and relevant differential diagnoses, and describes the treatment responses observed in each case. Diagnosing PAL is challenging, and its prognosis is generally poor. PAL should be considered in the differential diagnosis of adrenal masses, particularly in patients with a history of hypertension. Once diagnosed, management should

be guided by a multidisciplinary team specialized in adrenal and hematological disorders.

Introduction

Adrenal lymphoma is a rare clinical entity that is primarily classified into three categories: Primary adrenal lymphoma (PAL), which carries an estimated global incidence of 0.4-0.5 cases per million individuals per year, secondary adrenal lymphoma, and those cases involving simultaneous adrenal and extra-adrenal organ involvement. Among these, secondary adrenal lymphoma is the most common. PAL is exceedingly rare, accounting for <1% of all lymphoma cases, with <250 cases reported in the English literature to date (1). Common presenting symptoms of PAL include abdominal pain, fever, weight loss or signs of adrenal insufficiency, such as hypotension, skin hyperpigmentation, orthostatic hypotension and, in severe cases, adrenal crisis (2). However, adrenal insufficiency occurs in only ~50% of patients and generally manifests after destruction of >90% of adrenal tissues (3). Furthermore, due to its non-specific clinical features, imaging characteristics that frequently overlap with those of other adrenal tumors, and the usual absence of marked hormone hypersecretion, PAL is often misdiagnosed as adrenal metastasis or a 'non-functioning adrenal incidentaloma' (4). Notably, hypertension is a relatively common finding in patients with PAL, reported in 20-30% of cases across several case series, either as a pre-existing comorbidity or as a newly developed abnormality during disease progression (5-7); however, this association has not been systematically studied. The present report describes three cases of bilateral adrenal lymphoma, highlighting their imaging features and discussing relevant differential diagnostic considerations.

Case report

Case 1. An 83-year-old man was admitted to Zhuzhou Hospital Affiliated to Xiangya School of Medicine, Central South University (Zhuzhou, China) in October 2025, presenting with a 1-week history of poor appetite and bilateral lower limb weakness, accompanied by 5 kg of weight loss over

Correspondence to: Professor Lei Chen, Department of Urology, Zhuzhou Hospital Affiliated to Xiangya School of Medicine, Central South University, 116 Changjiang South Road, Zhuzhou, Hunan 412000, P.R. China
E-mail: 13607339924@163.com

Professor Yinchun Deng, First Department of Colorectal and Anal Surgery, Digestive Disease Medical Center Zhuzhou Hospital Affiliated to Xiangya School of Medicine, Central South University, 116 Changjiang South Road, Zhuzhou, Hunan 412000, P.R. China
E-mail: ydc20200509@163.com

*Contributed equally

Key words: adrenal gland, lymphoma, hypertension, diagnosis

the preceding month. The patient had a history of hypertension for >10 years, managed regularly with antihypertensive medications, with home blood pressure monitoring showing fluctuations around 140/90±10 mmHg. On admission, the temperature of the patient was 36.3°C and the blood pressure was 164/108 mmHg. During hospitalization, regular monitoring revealed blood pressure fluctuations around 155/105±10 mmHg. Laboratory tests demonstrated normal blood counts, with a serum sodium level of 132.7 mmol/l (normal range, 135-145 mmol/l), creatine kinase level of 38 U/l (normal range, 30-200 U/l), lactate dehydrogenase (LDH) level of 536 U/l (normal range, 135-225 U/l) and C-reactive protein level of 16.2 mg/l (normal range, <5 mg/l) (Table I). Based on the symptoms of the patient, a physical examination and the laboratory findings, contrast-enhanced abdominal computed tomography (CT) was performed, revealing bilateral adrenal masses, namely, a 5.5-cm lesion in the left adrenal gland and an ~3-cm lesion in the right adrenal gland (Fig. 1A). The patient underwent CT-guided biopsy, and histopathology with immunohistochemistry confirmed diffuse large B-cell lymphoma (pan-cytokeratin-negative, CD20-positive, CD79a-positive, CD3-negative, CD5-focally positive, CD56-negative, Bcl-2-strongly positive, MUM-1-positive, Bcl-6 ~70% and non-germinal center origin) (Fig. 2). A bone marrow biopsy demonstrated reduced cellularity, predominance of mature myeloid cells, a decreased erythroid ratio and absence of megakaryocytes. Considering the advanced age of the patient and comorbidities, the patient received one cycle of the POLA + R + miniCHP regimen (96 mg polatuzumab vedotin, day 0; 600 mg rituximab, day 1; 600 mg cyclophosphamide, day 2; 20 mg liposomal doxorubicin, day 2; 50 mg prednisone, days 2-6). Following this cycle, the patient was re-hospitalized due to sudden, persistent chest pain lasting 9 h. The patient's medical history included coronary artery stent implantation. Laboratory work-up revealed normal blood counts, negative troponin and creatine kinase, and a CRP level of 29.8 mg/l (normal, <5 mg/l), IL-6 level of 190.32 pg/ml (normal, <7 pg/ml) and IL-10 level of 16.94 pg/ml (normal, <10 pg/ml). The patient was unable to cooperate with breath-hold maneuvers, precluding a coronary CT angiography evaluation. CT showed partial regression of the previously enlarged mediastinal lymph node (Fig. 1B), and the blood pressure was maintained around 120/80±5 mmHg. Unstable angina was suspected rather than a reaction to the chemotherapy, and the patient improved after the anti-infective therapy that was administered due to the elevated inflammatory markers. Subsequently, the patient was administered the POLA + R + ibrutinib regimen (96 mg polatuzumab vedotin, day 0; 600 mg rituximab, day 1; 100 mg ibrutinib daily). Post-discharge, the patient completed four cycles of POLA + R + ibrutinib as an outpatient with each cycle lasting 21 days, with blood pressure fluctuations around 135/96±10 mmHg. The patient continues to be regularly followed up in the outpatient clinic every 6 months.

Case 2. A 73-year-old man was admitted to Zhuzhou Hospital Affiliated to Xiangya School of Medicine, Central South University, in September 2015, presenting with a 6-month history of intermittent dull abdominal pain. The past medical history included acute myocardial infarction

and hypertension; however, the patient had been taking medication irregularly and did not monitor their blood pressure. During hospitalization, the blood pressure fluctuated around 150/95±15 mmHg. Laboratory tests showed no significant abnormalities in complete blood count, liver or kidney function, or electrolytes. Abdominal CT revealed bilateral adrenal masses (right, 6.1x4.1 cm; left, 8.4x5.4 cm). The imaging differential diagnosis included metastasis or pheochromocytoma, among others (Fig. 1C). The patient underwent CT-guided biopsy, and histopathological and immunohistochemical analysis confirmed non-Hodgkin B-cell lymphoma (pan-cytokeratin-negative, CD20-positive, CD79a-positive, CD3-negative, CD5 focally positive, BCL-6 ~70%, MUM1-positive and non-germinal center origin) (Fig. 3). However, the patient refused any treatment. After 2 months, the patient was re-admitted with fatigue and night sweats. Laboratory investigations revealed a white blood cell count of 2.08x10⁹/l (normal range, 3.5-9.5x10⁹/l), a neutrophil count of 1.03x10⁹/l (normal range, 1.8-6.3x10⁹/l), a serum sodium level of 126.0 mmol/l (normal range, 135-145 mmol/l), a chloride level of 88.5 mmol/l (normal range, 96-106 mmol/l), an LDH level of 481 IU/l (normal range, 135-225 IU/l) and a α -hydroxybutyrate dehydrogenase level of 357 IU/l (normal range, 72-182 IU/l) (Table I). Repeat abdominal CT demonstrated enlargement of the bilateral adrenal masses compared with the CT performed 2 months ago (right, 7.3x4.7 cm; left, 9.6x6.2 cm) (Fig. 1D). The patient again declined further diagnostic workup or treatment. The patient has since passed away.

Case 3. A 63-year-old man was admitted to Zhuzhou Hospital Affiliated to Xiangya School of Medicine, Central South University, in September 2024, presenting with a decline in overall health, reporting 5 kg of weight loss over the past 2 months and generalized fatigue during the preceding month. Contrast-enhanced CT performed at a local hospital revealed bilateral adrenal masses and multiple enlarged retroperitoneal lymph nodes (Fig. 1E). Laboratory evaluation showed a white blood cell count of 3.37x10⁹/l (normal range, 3.5-9.5x10⁹/l), a reticulocyte percentage of 4.48% (normal range, 0.5-1.5%), a reticulocyte count of 0.11x10¹²/l (normal range, 0.024-0.084x10¹²/l), an LDH level of 2,369 U/l (normal range, 135-225 U/l) and a neuron-specific enolase level of 35.12 ng/ml (normal range, <16.3 ng/ml). Thyroid function tests, serum cortisol levels and catecholamine levels were within normal limits (Table I). ¹⁸F-fluorodeoxyglucose (FDG) positron emission tomography (PET) scanning demonstrated markedly increased FDG uptake in the enlarged adrenal glands [left adrenal gland maximum standardized uptake value (SUV_{max}), 16.5], as well as elevated metabolism in the hepatic hilum and retroperitoneum (Fig. 1F and G). To establish a definitive diagnosis, the patient underwent CT-guided biopsy, and histopathology confirmed diffuse large B-cell lymphoma of non-germinal center origin (pan-cytokeratin-negative, CD20-positive, CD79a-positive, CD3-negative, CD5 negative or minimally positive, BCL-2 strongly positive, BCL-6 positive in a high proportion of tumor cells and MUM1-positive) (Fig. 4). The patient received two cycles of R-CHOP chemotherapy (each cycle lasting 21 days), including 600 mg rituximab on

Table I. Patient clinical characteristics.

Parameters	Case 1	Case 2	Case 3
Age, years	83	73	63
Unilateral or bilateral	Bilateral	Bilateral	Bilateral
Adrenal insufficiency	Yes	Yes	Yes
Diagnostic procedure	Needle biopsy	Needle biopsy	Needle biopsy
Histological type	Diffuse large B-cell lymphoma (non-germinal center origin)	Diffuse infiltrative large B-cell lymphoma with small round cells	Diffuse large B-cell lymphoma (non-germinal center origin)
Immunohistochemistry	CD20(diffusely +), CD56(-),CK-pan(-), CD79α(+), CD3(-), CD5(few +), CD21(-), CD10(-), Bcl-2 (strongly +), Bcl-6 (~70% +)	CK-pan(-), CD45 (LCA)(+) ^a , Ki-67 (60% +) ^a , CD20(+), CD79α(+), CD3(-), CD5(+), CD10(-) ^a , Bcl-6(+), CD38(-) ^a , CD43(+) ^a	Ki-67(~90% +) ^a , CK7(-) ^a , CK-pan(-), CK20(-) ^a , CD20(+), CD3(-), CD38(-) ^a , CD21(-) ^a , CD10(-) ^a , Bcl-6(+), Bcl-2(+)
Treatment	Chemotherapy	N/A	Chemotherapy
Treatment outcome	Partial response	N/A	Partial response
Mean BP before admission, mmhg	155/105±10	150/95±15	140/90±10
Mean BP after treatment, mmhg	120/80±5	N/A	125/85±6
Hemoglobin, g/dl	102	78	88
White blood cells, g/l	4.22	2.08	3.37
CRP, mg/dl	16.2	77.7	30.1
LDH, U/l	536	481	2369
Cortisol, μg/dl	N/A	N/A	15
Urinary cortisol, μg/24 h	N/A	N/A	9.6
Aldosterone/renin activity ratio	N/A	N/A	7.77
α-hydroxybutyrate dehydrogenase, U/l	N/A	N/A	357

^aResult derived from the original pathological report; representative histological slides were not retained for re-imaging. CK, cyokeratin; BP, blood pressure; CRP, C-reactive protein; LDH, lactate dehydrogenase; N/A, not available (test not performed).

day 1, 1.17 g cyclophosphamide on day 1, 2 mg vincristine on day 1 and 100 mg prednisone on days 1-5. Follow-up CT revealed marked regression of multiple lymphadenopathies. Subsequently, the patient received three additional cycles of R-CHOP. Routine monitoring, including tumor markers, complete blood count, and liver and kidney function tests, showed no significant abnormalities. The patient commenced three cycles of rituximab targeted therapy (600 mg on day 1 of each 28-day cycle) as an outpatient, starting in December 2024, with follow-up CT showing no apparent abnormalities (Fig. 1H) and blood pressure fluctuations around 138/88±6 mmHg. Following the three cycles of rituximab-based chemotherapy, the patient was scheduled for routine outpatient follow-up every 3 months, including blood tests and blood pressure monitoring. An annual follow-up CT scan was also planned. During the follow-up visits, the patient's blood pressure remained within normal limits and no significant abnormalities were detected on

blood tests. However, the patient declined the recommended follow-up CT scan and, notably, has not attended any further appointments since June 2025.

Methods

Histopathology. For the hematoxylin and eosin (H&E) staining of the adrenal biopsy specimen in case 1, the histopathological features indicating the diagnosis included a dense, diffuse proliferation of large, atypical lymphoid cells that replace the normal adrenal architecture. These neoplastic cells exhibit large irregular nuclei, vesicular chromatin, prominent nucleoli and scant cytoplasm, consistent with high-grade lymphoma. For all cases presented, the biopsy or surgical tissue specimens were immediately fixed in 10% neutral buffered formalin at room temperature (20-25°C) for 12 to 24 h. The fixed tissues were subsequently dehydrated, embedded in paraffin and cut into 4-μm thick sections. The sections were routinely stained with H&E at room

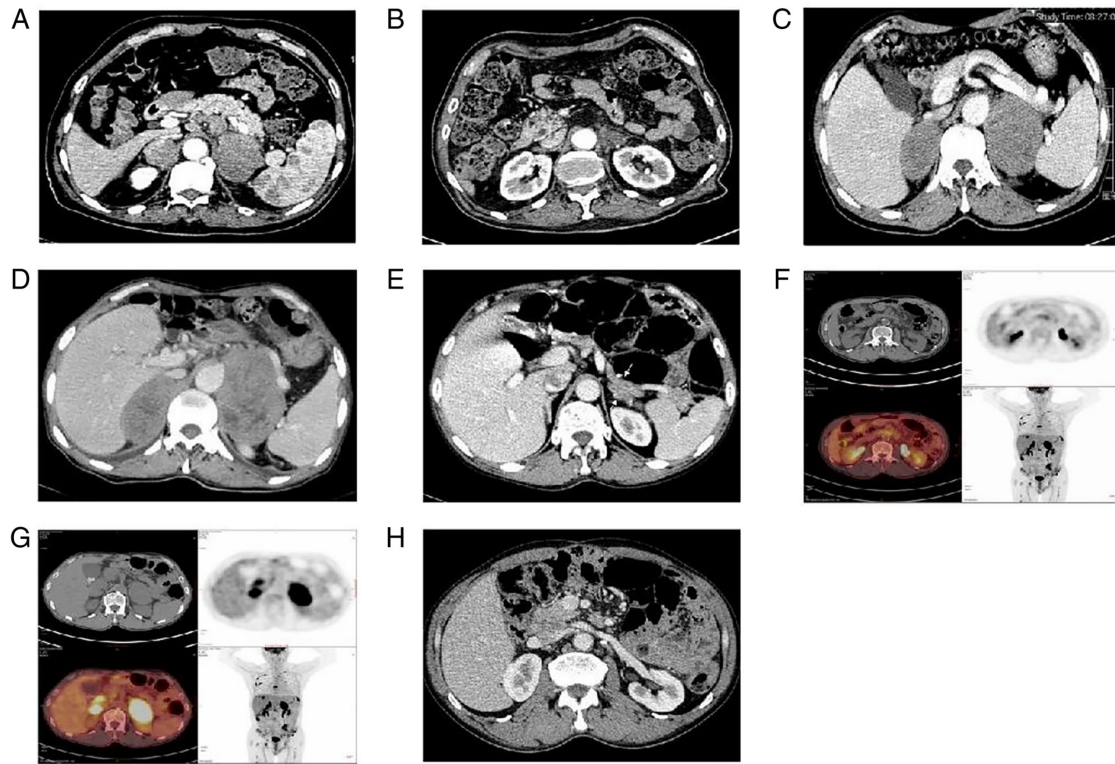


Figure 1. (A) Initial CT scan showing bilateral adrenal masses, with a 5.5-cm lesion in the left adrenal gland and a ~3-cm lesion in the right adrenal gland. (B) Follow-up imaging demonstrating multiple enlarged mediastinal lymph nodes and partial regression of the adrenal masses. (C) CT scan revealing progression of adrenal lesions, measuring 6.1x4.1 cm on the right and 8.4x5.4 cm on the left. (D) Subsequent imaging showing further enlargement of the bilateral adrenal masses compared with prior scans. (E) CT demonstrating bilateral adrenal masses and multiple enlarged retroperitoneal lymph nodes. (F and G) Different axial levels of the same FDG PET/CT examination. (F) Scan obtained at the renal hilar level demonstrating prominent FDG activity within the bilateral renal collecting systems, which is mainly consistent with physiological urinary excretion of FDG. No definite focal renal parenchymal hypermetabolic lesion is clearly identified on this slice. By contrast, the scan in (G) was obtained at a more cranial upper-abdominal level, where focal hypermetabolic activity is more evident in the adrenal/upper retroperitoneal region, with additional increased FDG uptake around the hepatic hilar or retroperitoneal area. Therefore, (F) mainly reflects urinary tracer excretion at the renal level, whereas (G) better demonstrates pathological FDG-avid lesions involving the adrenal and adjacent retroperitoneal regions. (H) At the renal hilar level, contrast-enhanced CT demonstrates no significant abnormalities, with incidental mild thickening of the left adrenal gland.

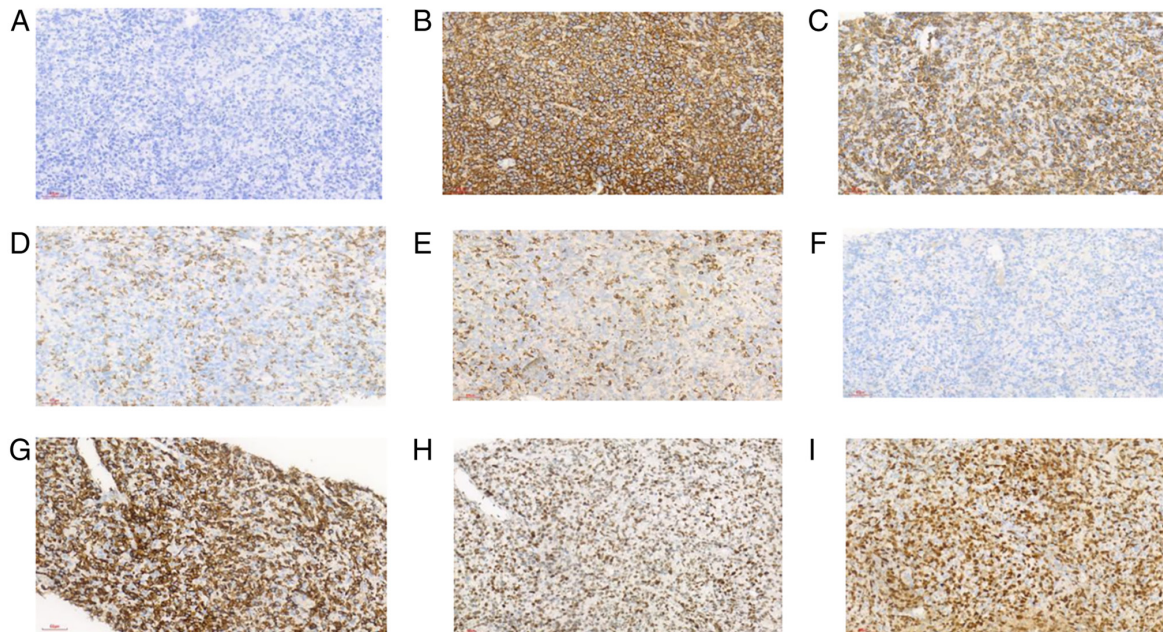


Figure 2. Immunohistochemical features of the tumor in case 1. Immunohistochemical staining demonstrates (A) negative expression for pan-cytokeratin (magnification, x200), (B) positive expression for CD20 (magnification, x200) and (C) CD79a (magnification, x200), and (D) negative expression for CD3 (magnification, x200). (E) CD5 (magnification, x200) shows focal positivity, whereas (F) CD56 (magnification, x200) is negative. The tumor cells exhibit (G) strong Bcl-2 (magnification, x200) expression, with (H) Bcl-6 (magnification, x200) positivity in ~70% of cells and (I) MUM1-positive expression.

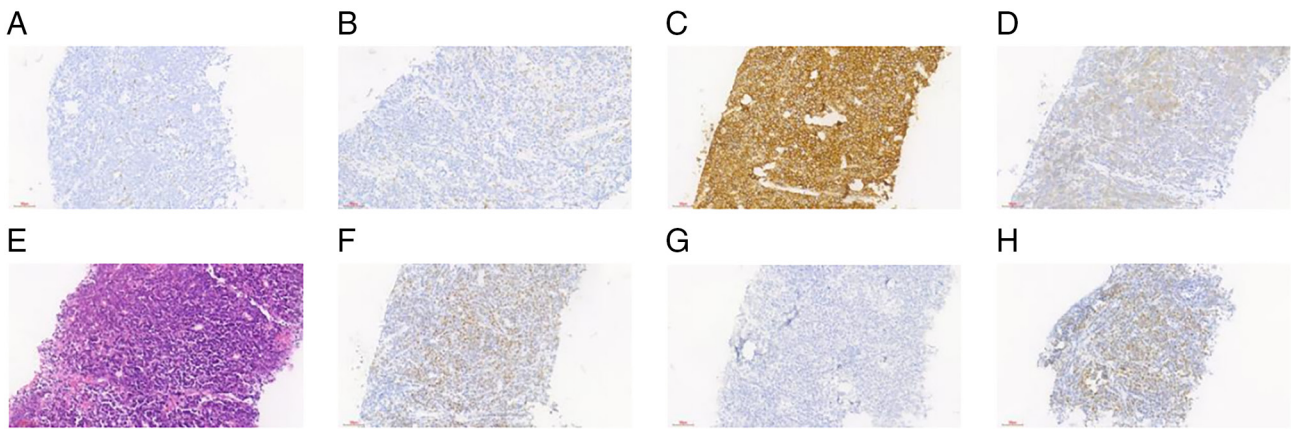


Figure 3. Histopathological and immunohistochemical features of the lesion in case 2. Immunohistochemical staining showed that the tumor cells were (A) negative for CD3 (magnification, x200), with only scattered background reactive T lymphocytes observed, (B) focally positive for CD5 (magnification, x200), (C) diffusely and strongly positive for CD20 (magnification, x200), and (D) positive for CD79a (magnification, x200). (E) Hematoxylin and eosin staining demonstrated diffuse infiltration of densely packed lymphoid cells with partial architectural effacement (magnification, x200). (F) Additional immunohistochemical staining revealed BCL-6 (magnification, x200) positivity in ~70% of tumor cells, (G) negative expression for pan-cytokeratin (magnification, x200), and (H) positive nuclear expression of MUM1 (magnification, x200).

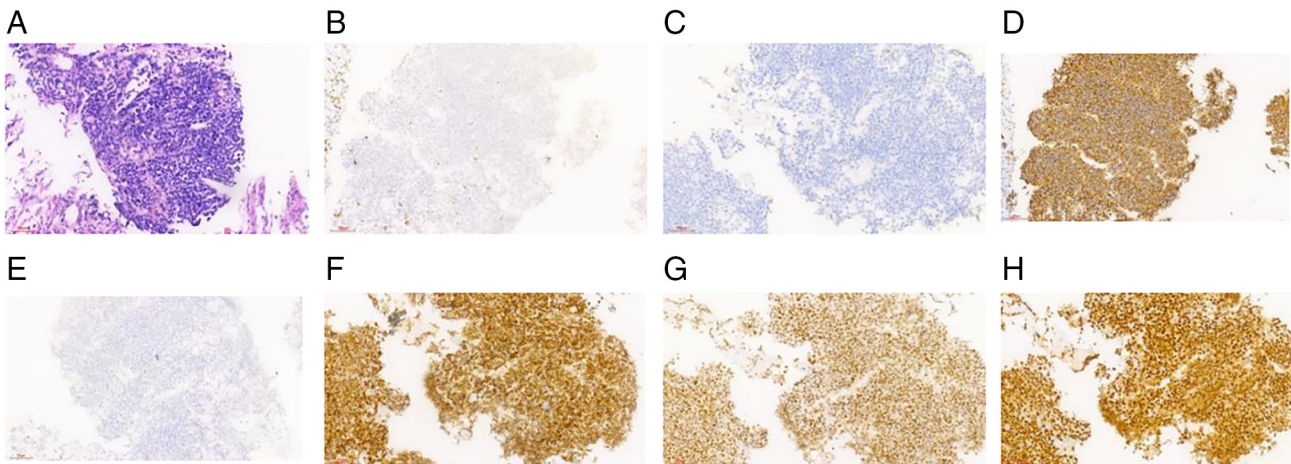


Figure 4. Histopathological and immunohistochemical features of the lesion in case 3. (A) Hematoxylin and eosin staining demonstrated diffuse infiltration of densely packed small- to medium-sized lymphoid cells with architectural effacement (magnification, x200). Immunohistochemical staining showed that the (B) tumor cells were negative for CD3 (magnification, x200), with only scattered background reactive T lymphocytes observed, and (C) negative or only minimally positive for CD5 (magnification, x200). (D) The tumor cells were diffusely and strongly positive for CD20 (magnification, x200), whereas (E) pan-cytokeratin (magnification, x200) expression was negative. Additional immunohistochemical staining revealed (F) strong diffuse expression of BCL-2 (magnification, x200), (G) positive expression of BCL-6 (magnification, x200) in a high proportion of tumor cells and (H) positive nuclear expression of MUM1 (magnification, x200).

temperature (with a staining duration of ~5 min for hematoxylin and 1-2 min for eosin) following standard institutional laboratory protocols. The histological slides were examined and imaged using a standard bright-field light microscope. All representative microphotographs are provided with a definitive scale bar (60 μm) directly embedded within the images to indicate magnification.

Immunohistochemistry (IHC). All immunohistochemical staining was performed on formalin-fixed, paraffin-embedded tissue specimens. The tissues were fixed in 10% neutral buffered formalin at room temperature (20-25°C) for 12 to 24 h and embedded in paraffin resin. Tissue blocks were sectioned at a thickness of 4 μm . Following deparaffinization and rehydration, antigen retrieval was performed. Endogenous peroxidase activity was blocked using 3% hydrogen peroxide for 10 min

at room temperature. Non-specific binding was blocked using 5% bovine serum albumin (Beijing Zhongshan Jinqiao Biotechnology Co., Ltd.) at room temperature for 30 min. The sections were then incubated with primary antibodies against various markers (including Bcl-2, Bcl-6, CD56, pan-CK and CD5; Table II) at 4°C overnight. Following primary incubation, the sections were incubated with a horseradish peroxidase-conjugated secondary antibody system (Table II) at room temperature for 30 min. The signal was visualized using 3,3'-diaminobenzidine chromogen, resulting in a brown precipitate, followed by counterstaining with hematoxylin. All IHC slides were evaluated and captured using a standard bright-field light microscope. A definitive scale bar (60 μm) is provided in the lower-left corner of all representative IHC figures.

Table II. Antibody details.

Antibody	Supplier	Clone	Catalog number	Dilution
Primary				
Bcl-2	Roche Diagnostics GmbH	SP66	92-790-4604	Ready-to-use
Bcl-6	Beijing Zhongshan Jinqiao Biotechnology Co., Ltd.	LN22	ZM-0057	1:100
CK-Pan	Fuzhou Maixin Biotechnology Development Co., Ltd.	AE1/AE3	Kit 0009	Ready-to-use
CD3	Fuzhou Maixin Biotechnology Development Co., Ltd.	MX036	MAB-0740	Ready-to-use
CD5	Fuzhou Maixin Biotechnology Development Co., Ltd.	MX052	MAB-0827	Ready-to-use
CD20	Beijing Zhongshan Jinqiao Biotechnology Co., Ltd.	L26	ZM-0039	1:200
CD56	Beijing Zhongshan Jinqiao Biotechnology Co., Ltd.	UMAB83	ZM-0057	1:100
CD79a	Beijing Zhongshan Jinqiao Biotechnology Co., Ltd.	EP82	ZA-0293	1:100
Mum-1	Beijing Zhongshan Jinqiao Biotechnology Co., Ltd.	EP190	ZA-0583	1:100
Secondary				
HRP-Polymer Anti-Mouse/ Rabbit IgG	Beijing Zhongshan Jinqiao Biotechnology Co., Ltd.	N/A	PV-9000	Ready-to-use

Discussion

Adrenal lymphoma is a rare form of extranodal lymphoma. Among patients with non-Hodgkin lymphoma, adrenal involvement occurs in ~24% of cases; however, PAL accounts for only ~3% of all extranodal lymphomas (8). PAL predominantly affects male patients, with a male-to-female ratio of ~7:1 and a median age at onset of ~68 years (8). All 3 patients in the present case series were male, with a mean age at diagnosis of 73 years, which is consistent with the literature (7). PAL often presents with bilateral adrenal involvement, and primary adrenal insufficiency develops in 50-70% of patients with bilateral disease (9). Clinically, the most common manifestations are systemic 'B symptoms', including fever, night sweats and unexplained weight loss, which are characteristic of aggressive lymphomas. In addition, due to the mass effect of the tumor, patients frequently experience abdominal or lumbar back distension and pain. Furthermore, the most distinctive clinical features arise from adrenocortical insufficiency itself, and may include orthostatic hypotension, fatigue, nausea, vomiting and skin hyperpigmentation, among others (10).

The etiology and pathogenesis of PAL have not been fully elucidated, as the human adrenal gland lacks native lymphoid tissue. Some researchers have proposed that PAL may arise in the context of pre-existing autoimmune adrenalitis (11). Alternatively, others have suggested that the tumor may originate from residual hematopoietic tissue within the adrenal gland, analogous to extranodal extramedullary hematopoietic foci (12). Despite differences in these hypotheses regarding tumor origin, immune dysfunction is considered to be an important predisposing factor (10).

The diagnosis of PAL is often challenging. Firstly, its clinical symptoms and signs are largely non-specific. Secondly, conventional imaging modalities, such as CT and MRI, often lack distinctive features. On CT, PAL typically presents as bilateral adrenal masses with heterogeneous internal density, occasionally with areas of necrosis or hemorrhage, whereas a minority of cases may exhibit homogeneous

lesions (13). MRI usually shows lesions with low signal intensity on T1-weighted images and predominantly high signal intensity on T2-weighted images, with some lesions exhibiting mixed-signal areas (14). PET and PET-CT, based on increased glucose metabolism in malignant tumors, can aid in distinguishing PAL from secondary adrenal tumors, such as metastases. Studies have indicated that on non-contrast CT, an attenuation value >10 HU should raise suspicion for malignancy (15-17). Such lesions generally exhibit increased FDG uptake on PET/CT. An SUV_{max} value >2.5 is generally considered indicative of possible malignancy (18). However, SUVs are influenced by multiple factors, including body weight, blood glucose level, and the interval between tracer injection and imaging. Therefore, calculating the SUV ratio between the adrenal gland and liver, rather than relying solely on the adrenal SUV_{max} , provides a more stable measure of metabolic differences, thereby improving the accuracy of distinguishing benign from malignant adrenal tumors (10).

Histopathological examination is essential for determining the nature of an adrenal tumor. This is typically achieved through CT- or ultrasound (US)-guided core needle biopsy, or by pathological evaluation following surgical resection of the mass. However, unlike in patients with other adrenal tumors, in patients with PAL, surgical resection is primarily reserved for obtaining a definitive diagnosis or for cytoreductive therapy in cases of localized disease progression (7). Consequently, the role of surgery in the management of PAL remains controversial. Grigg and Connors (19) noted that surgical resection alone does not improve outcomes and that optimal management relies on systemic chemotherapy, suggesting that surgery may be associated with a poor prognosis when used as the primary modality. Surgical intervention should be considered if the tumor is small, located in a position unfavorable for percutaneous biopsy, or if the patient is at high risk of complications. For example, surgery is appropriate when the tumor is inaccessible via a safe percutaneous route, or when a percutaneous biopsy fails to provide sufficient tissue for

a definitive diagnosis (20). Conversely, if surgical access is unlikely to yield adequate tissue samples, priority should be given to a US- or CT-guided biopsy.

Treatment strategies for PAL primarily include chemotherapy, adrenalectomy, radiotherapy or combinations thereof. Standard chemotherapy regimens include CHOP, R-CHOP, CHOP with prednisolone, CVP (cyclophosphamide, vincristine and prednisone) and MACOP-B (cyclophosphamide, doxorubicin, prednisone, methotrexate and bleomycin), among others (10). Studies have demonstrated that the addition of rituximab to CHOP (forming R-CHOP) can improve overall survival. For example, Kim *et al* (21) reported a 2-year overall survival rate of 68.3% and a complete response rate of 54.8% in patients receiving this regimen. Another study involving 28 patients with PAL indicated that 64% received CHOP, 50% received R-CHOP and 18% received combination chemotherapy containing doxorubicin, cyclophosphamide, vindesine, bleomycin and prednisone. The overall survival rate for the entire cohort was 61.6%. Notably, survival reached 100% in patients who underwent autologous hematopoietic stem cell transplantation, suggesting that this therapy may contribute to a prolonged survival time (22). In the present case series, in case 1, due to an advanced age and multiple comorbidities, the patient was treated with the POLA + R + miniCHP regimen. In case 2, the patient declined systemic therapy, whereas the patient in case 3 is currently undergoing R-CHOP chemotherapy. Therapeutic decision-making for PAL is often complex. Following diagnosis, evaluation by experienced specialists in the fields of hematology and oncology is required to formulate an individualized treatment plan tailored to the condition of the patient. Overall, the prognosis of patients with PAL is poor. Several clinical factors are associated with worse outcomes, including older age at diagnosis, larger tumor size, coexisting renal insufficiency and elevated LDH levels (6,23). A pooled analysis by Singh *et al* (24) of 69 patients with PAL, encompassing clinical features, pathological findings, treatment regimens and outcomes, revealed a generally poor prognosis, with a complete response rate of 43% and a long-term survival rate of 22%. Among 49 patients with definitive outcome data, 36 died from disease progression and 2 died from chemotherapy-related toxicity. A systematic review by Rashidi and Fisher (7) in 2013, which included 187 PAL cases, reported survival rates of 67, 46 and 20% at 3, 6 and 12 months, respectively. Survival rates were even lower for patients with central nervous system involvement, at 62, 46 and 8% for the corresponding time points.

The clinical evaluation of an adrenal mass requires consideration of a broad differential diagnosis and the appropriate investigative tests. The diagnostic algorithm for unilateral and bilateral adrenal masses summarized by Spyroglou *et al* (10) recommends beginning with the patient's initial clinical manifestations and signs, followed by sequential laboratory and imaging studies for stepwise exclusion and a definitive diagnosis. In clinical practice, the diagnostic approach for an adrenal mass coexisting with hypertension relies heavily on endocrine functional assessment. For example, primary aldosteronism typically requires screening of the aldosterone/renin ratio, whereas the diagnosis of pheochromocytoma depends on the measurement of plasma or urinary catecholamines and their metabolites. This hormone-focused

approach exhibits high diagnostic efficacy for functional adrenal tumors. By contrast, the vast majority of PAL cases are not associated with significant hormone hypersecretion. Hypertension in these patients is often attributed to essential hypertension, age or comorbidities, rather than being directly linked to the tumor. This diagnostic bias is a key factor contributing to the high rate of missed PAL diagnoses in hypertensive populations. Notably, the co-occurrence of PAL and hypertension is an extremely rare clinical entity. While a precise epidemiological rate cannot be determined, this phenomenon has been documented in multiple isolated case reports (5,7,25). Some patients have a long-standing history of hypertension prior to the diagnosis of PAL, whereas others develop new-onset or worsening hypertension during tumor progression. Furthermore, literature reports indicate that the blood pressure may exhibit dynamic changes during treatment, often improving markedly following chemotherapy, immunotherapy or surgery (9,26,27). In the present case series, 2 patients had a confirmed history of hypertension prior to admission. However, during the period of PAL diagnosis, monitoring revealed that their blood pressure was elevated compared with their usual baseline. For example, in case 1, blood pressure fluctuated around 155/105±10 mmHg during hospitalization before initiating POLA + R + miniCHP chemotherapy, and stabilized around 120/80±5 mmHg following treatment. Notably, hormone levels such as serum epinephrine and norepinephrine levels were not assessed at that time. The other patient in case 2 did not undergo any further therapy or systematic monitoring.

The present study has several limitations. First, PAL is extremely rare, and cases coexisting with hypertension are even more uncommon. Conclusions drawn from small samples or case reports may be coincidental, and their generalizability, as well as the specific association between hypertension and PAL, requires validation in large-scale prospective studies. Second, although the coexistence of hypertension and PAL has been observed, a definitive causal relationship has not been established. Hypertension may result from direct tumor effects (such as renal vascular compression) or a systemic inflammatory state, or may represent an independent comorbid condition. Currently, there is a lack of systematic prospective blood pressure monitoring and studies on blood pressure dynamics following tumor resection; therefore, the underlying mechanisms remain unclear.

In summary, PAL is a rare disease; however, its detection rate appears to be increasing with advances in imaging and pathological diagnostic techniques. In patients presenting with an adrenal mass and concomitant hypertension, PAL should be considered in the differential diagnosis alongside functional adrenal tumors. Increased clinical vigilance for this condition may help reduce missed or incorrect diagnoses, potentially improving patient outcomes.

Acknowledgements

Not applicable.

Funding

No funding was received.

Availability of data and materials

The data generated in the present study may be requested from the corresponding author.

Authors' contributions

KT, ZH, MT and YZ collected the clinical, imaging and pathological data of the patient, and wrote the manuscript. LC and YD conceived and designed the study, and revised the manuscript. LC and YD confirm the authenticity of all the raw data. All authors have read and approved the final version of the manuscript.

Ethics approval and consent to participate

Not applicable.

Patient consent for publication

Written informed consent was obtained from the patients for publication of the images and data.

Competing interests

The authors declare that they have no competing interests.

References

- Ahmed TM, Fishman EK, Morris-Wiseman LF, Baraban E and Chu LC: Cinematic rendering of primary adrenal lymphoma. *Curr Probl Diagn Radiol* 53: 641-647, 2024.
- Dobrinja C, Trevisan G and Liguori G: Primary bilateral adrenal Non-Hodgkin's Burkitt-Like lymphoma: A rare cause of primary adrenal insufficiency. Case report and literature review. *Tumori* 93: 625-630, 2007.
- Ercolak V, Kara O, Gunaldi M, Usul Afsar C, Bozkurt Duman B, Acikalin A, Ergin M and Erdođan Ş: Bilateral primary adrenal non-hodgkin lymphoma. *Turk J Haematol* 31: 205-206, 2014.
- Kłosowski P, Brzezińska N, Kmieć P, Okroj D, Zembruska S, Kujawa M, Babińska A and Świątkowska-Stodulska R: Primary adrenal lymphoma and its mimics: Clinico-radiological differential diagnosis. *Front Endocrinol (Lausanne)* 16: 1639878, 2025.
- Wang Q, Cao X, Jiang J, Wang T and Jin MS: Bilateral primary adrenal lymphoma accompanying hypertension. *Urology* 79: e27-e28, 2012.
- Zeng J, Yan F, Chen Y, Zang L, Chen K, Lyu Z, Dou J, Mu Y, Lin M and Yang G: Primary adrenal lymphoma: Two case series from China. *Front Endocrinol (Lausanne)* 12: 778984, 2022.
- Rashidi A and Fisher SI: Primary adrenal lymphoma: A systematic review. *Ann Hematol* 92: 1583-1593, 2013.
- Kumar R, Xiu Y, Mavi A, El-Haddad G, Zhuang H and Alavi A: FDG-PET imaging in primary bilateral adrenal lymphoma: A case report and review of the literature. *Clin Nucl Med* 30: 222-230, 2005.
- Wang JP, Sun HR, Li YJ, Bai RJ and Gao S: Imaging features of primary adrenal lymphoma. *Chin Med J (Engl)* 122: 2516-2520, 2009.
- Spyroglou A, Schneider HJ, Mussack T, Reincke M, von Werder K and Beuschlein F: Primary adrenal lymphoma: 3 case reports with different outcomes. *Exp Clin Endocrinol Diabetes* 119: 208-213, 2011.
- Ellis RD and Read D: Bilateral adrenal non-Hodgkin's lymphoma with adrenal insufficiency. *Postgrad Med J* 76: 508-509, 2000.
- Reddy SV, Prabhudesai S and Gnanasekaran B: Origin of primary adrenal lymphoma and predisposing factors for primary adrenal insufficiency in primary adrenal lymphoma. *Indian J Endocrinol Metab* 15: 350-351, 2011.
- Alvarez-Castells A, Pedraza S, Tallada N, Castella E, Gifre L and Torrents C: CT of primary bilateral adrenal lymphoma. *J Comput Assist Tomogr* 17: 408-409, 1993.
- Kato H, Itami J, Shiina T, Uno T, Arimizu N, Fujimoto H, Mikata A, Tamaru J and Araki A: MR imaging of primary adrenal lymphoma. *Clin Imaging* 20: 126-128, 1996.
- Hamrahan AH, Ioachimescu AG, Remer EM, Motta-Ramirez G, Bogabathina H, Levin HS, Reddy S, Gill IS, Siperstein A and Bravo EL: Clinical utility of noncontrast computed tomography attenuation value (hounsfield units) to differentiate adrenal adenomas/hyperplasias from nonadenomas: Cleveland Clinic experience. *J Clin Endocrinol Metab* 90: 871-877, 2005.
- Boland GW, Lee MJ, Gazelle GS, Halpern EF, McNicholas MM and Mueller PR: Characterization of adrenal masses using unenhanced CT: An analysis of the CT literature. *AJR Am J Roentgenol* 171: 201-204, 1998.
- Fassnacht M, Arlt W, Bancos I, Dralle H, Newell-Price J, Sahdev A, Tabarin A, Terzolo M, Tsagarakis S and Dekkers OM: Management of adrenal incidentalomas: European Society of Endocrinology Clinical Practice Guideline in collaboration with the European Network for the Study of Adrenal Tumors. *Eur J Endocrinol* 175: G1-G34, 2016.
- Jeong YJ, Yoon HJ, Kang DY and Park KW: Quantitative comparative analysis of amyloid PET images using three radio-pharmaceuticals. *Ann Nucl Med* 37: 271-279, 2023.
- Grigg AP and Connors JM: Primary adrenal lymphoma. *Clin Lymphoma* 4: 154-160, 2003.
- Sharma KV, Venkatesan AM, Swerdlow D, DaSilva D, Beck A, Jain N and Wood BJ: Image-guided adrenal and renal biopsy. *Tech Vasc Interv Radiol* 13: 100-109, 2010.
- Kim YR, Kim JS, Min YH, Hyunyeon D, Shin HJ, Mun YC, Park Y, Do YR, Jeong SH, Park JS, *et al*: Prognostic factors in primary diffuse large B-cell lymphoma of adrenal gland treated with rituximab-CHOP chemotherapy from the Consortium for Improving Survival of Lymphoma (CISL). *J Hematol Oncol* 5: 49, 2012.
- Laurent C, Casasnovas O, Martin L, Chauchet A, Ghesquieres H, Aussedat G, Fornecker LM, Bologna S, Borot S, Laurent K, *et al*: Adrenal lymphoma: Presentation, management and prognosis. *QJM* 110: 103-109, 2017.
- Ekhzaimy A and Mujamammi A: Bilateral primary adrenal lymphoma with adrenal insufficiency. *BMJ Case Rep* 2016: bcr2016217417, 2016.
- Singh D, Kumar L, Sharma A, Vijayaraghavan M, Thulkar S and Tandon N: Adrenal involvement in non-Hodgkin's lymphoma: Four cases and review of literature. *Leuk Lymphoma* 45: 789-794, 2004.
- Feldberg MA, Hendriks MJ and Klinkhamer AC: Massive bilateral non-Hodgkin's lymphomas of the adrenals. *Urol Radiol* 8: 85-88, 1986.
- Lee EY, Kim KM, Kim KJ, Noh S, Kim JS, Yang W and Lim SK: Primary Bilateral Adrenal Non-Hodgkin's Lymphoma Presented with Adrenal Insufficiency: A Case Report. *Endocrinol Metab* 26: 101-105, 2011.
- Kim KM, Yoon DH, Lee SG, Lim SN, Sug LJ, Huh J and Suh C: A case of primary adrenal diffuse large B-cell lymphoma achieving complete remission with rituximab-CHOP chemotherapy. *J Korean Med Sci* 24: 525-528, 2009.



Copyright © 2026 Tan et al. This work is licensed under a Creative Commons Attribution-NonCommercial-NoDerivatives 4.0 International (CC BY-NC-ND 4.0) License.